

Study of Red-Emission Piezochromic Materials Based on Triphenylamine

Chunxuan Qi, Hengchang Ma,* Hongting Fan, Zengming Yang, Haiying Cao, Qiaojuan Wei, and Ziqiang Lei*^[a]

Two conjugated molecules based on triphenylamine and 1,3-indandione have been synthesized by employing Knoevenagel condensation. Both materials demonstrated aggregation-induced emission behavior, and solvato- and piezochromic prop-

erties. These red luminescence materials are able to respond to F⁻ and I⁻ sensitively. The emission wavelength changed by almost 100 nm in the presence of F⁻ and I⁻, and could be observed by the naked eye under daylight and UV light.

Introduction

Organic luminescent materials with unique and excellent optoelectronic properties have attracted much attention as a result of their wide applications as biological^[1] or chemical probes,^[2] photoelectric materials,^[3] or piezoluminescence sensors.^[4] In most cases, the emission is quenched when the fluorescent molecules aggregate, as caused by the aggregation-caused quenching (ACQ) effect. According to reports in the literature, molecules in the aggregated state suffer from short-range interactions, such as π - π stacking, which leads to fluorescence quenching, and thus, restricts further applications.^[5] Fortunately, in 2001, Tang's group reported two new fluorogen species: 2,3,4,5-tetraphenylsilole (TPS) and tetraphenylethene (TPE).^[6] These molecules are weakly emissive in dilute solution, but have a strong emission as aggregates or in the solid state. This phenomenon is called the aggregation-induced emission (AIE) effect. This effect is mainly ascribed to restricted intramolecular rotation (RIR): in solution, phenyl rings in TPS or TPE can freely rotate. However, in the aggregated state, intramolecular rotations are greatly restricted, so TPS and TPE cannot accumulate through a π - π stacking process. Thus, fluorescence emission emerges.^[7]

Piezochromic (mechanochromic) luminescent materials have been explored in recent years,^[8] because of great potential applications in mechanical sensors, security systems, deformation detectors, optical memories, and some kinds of display devices.^[4b,e,9] However, mechanochromic luminescent materials are seldom discussed; this may be attributed to the fact that a common synthetic protocol for mechanochromic compounds is not clear and the ACQ effect. TPE and triphenylamine (TPA) are two kinds of ideal luminescent cores. Some kinds of mechanochromic molecules have been reported, such as TPE sub-

stituted with 1,3-indandione (IND-TPE).^[4a] Because TPA is a core with ACQ properties, most TPA-based derivatives exhibit ACQ properties, which limits their applications.^[10] However, it should be noted that several examples of decorated TPA derivatives show emission behavior that has changed from ACQ to AIE; this provides the possibility of designing and preparing AIE-active TPA derivatives.^[11]

Although F⁻ is an essential element for dental health and the treatment of osteoporosis,^[12] excessive ingestion of fluoride may cause kidney disorders, fluorosis, urolithiasis, and even cancer or death.^[13] Therefore, it is very meaningful to develop fluorescent probes that are able to show high sensitivity,^[12c,14] rapid response,^[12c,15] and easy to observe^[12b,14b,16] toward F⁻ ion detection. Recently, there were three representative strategies for F⁻ recognition: 1) fluoride-ion-induced deprotonation through hydrogen bonding,^[14a,15b,17] 2) forming B-F compounds,^[12b,17b] and 3) destroying Si-O or Si-C bonds through desilylation.^[15a,16a,18] The desilylation reaction needs excessive F⁻ and B-F compounds are sensitive to oxygen.^[19] Tetrabutylammonium fluoride (TBAF) is a common organic base and promotes the hydrolysis reaction of olefins, which are replaced by electron-withdrawing substituents. At the same time, iodide is of great interest owing to its essential role for thyroid gland function.^[20] Herein, we report two kinds of red-emission materials, which have AIE and piezochromic properties (Scheme 1). Both of them can be used to recognize F⁻ and I⁻ ions in THF, which could be easily detected by the naked eye under visible- and UV-light illumination.

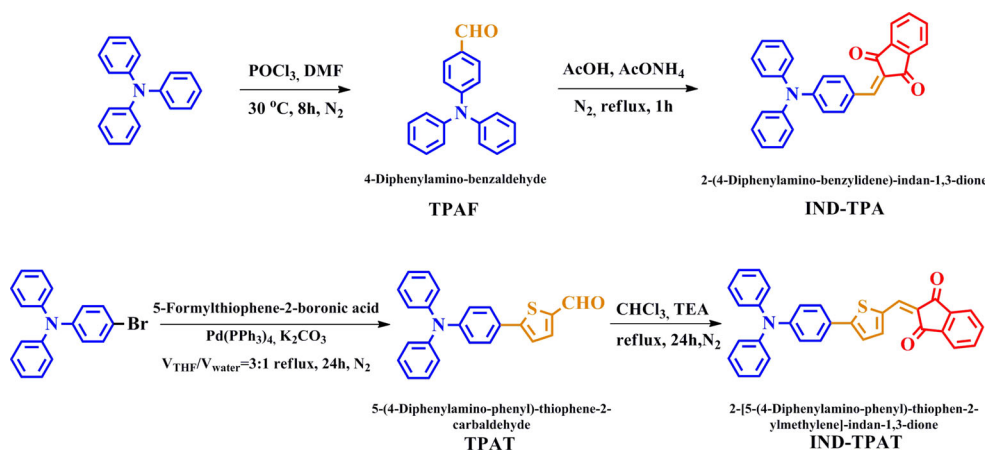
Results and Discussion

Solvatochromism

It is known that TPA is usually an electron donor and IND is regarded as an electron acceptor. So, 2-(4-Diphenylaminobenzylidene)indan-1,3-dione (IND-TPA) or 2-[5-(4-diphenylaminophenyl)thiophen-2-ylmethylene]indan-1,3-dione (IND-TPAT) have electron pull-push properties and may result in intramolecular

[a] C. Qi, Prof. H. Ma, H. Fan, Z. Yang, H. Cao, Q. Wei, Prof. Z. Lei
Chemistry Department, Northwest Normal University
967 Anning East Road, Lanzhou 730070 (P. R. China)
E-mail: mahczju@hotmail.com
leizq@nwnu.edu.cn

Supporting information for this article can be found under <http://dx.doi.org/10.1002/cplu.201600104>.



Scheme 1. Synthetic routes to IND-TPA and IND-TPAT.

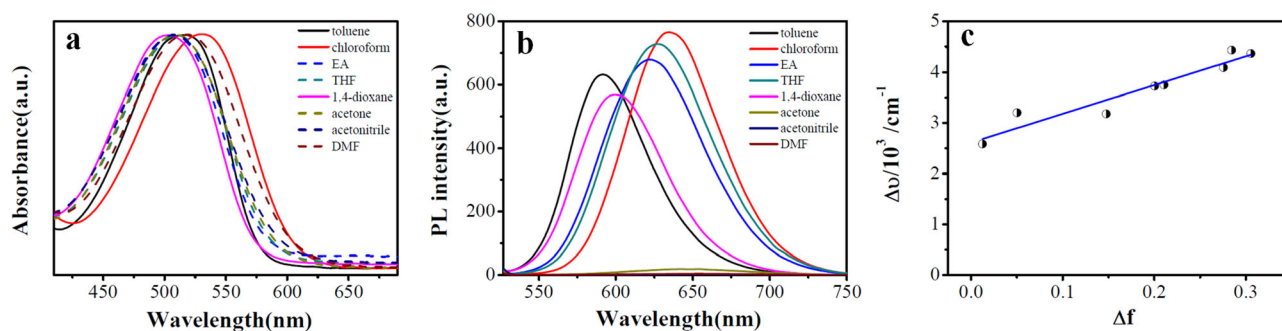


Figure 1. a) Absorption spectra of IND-TPAT in different solvents. b) PL spectra of IND-TPAT in different solvents. c) Plot of Stokes shift ($\Delta\nu$) of IND-TPAT in each solvent versus Δf of the respective solvent. Concentration: 20 μM . Solvents: toluene, chloroform, ethyl acetate (EA), THF, 1,4-dioxane, acetone, acetonitrile, dimethylformamide (DMF).

charge transfer (ICT). Thus, the absorption and emission behavior of IND-TPA and IND-TPAT in solution are probably related to the solvent polarity.^[21]

To study the solvatochromic behavior of IND-TPAT and IND-TPA, the UV/Vis absorption and fluorescence spectra are performed in different polarity solvents. From Figure 1, we can see that the UV/Vis absorption changes negligibly with solvents of different polarities. However, under the same measurement conditions, the IND-TPAT and IND-TPA fluorescence spectra changed clearly from less polar toluene to more polar DMF (Figure 1 b and Figure S1 in the Supporting Information); these results demonstrate a typical solvatochromic effect. The photoluminescence (PL) intensity is gradually reduced with increasing solvent polarity. The fluorescence quantum yield (Φ_f) decreases from 0.89 to 0.01% for IND-TPA and from 1.4 to 0.01% for IND-TPAT when the solvent is changed from toluene to DMF (Tables S1 and S2 in the Supporting Information). The large redshift, combined with the decreased value of Φ_f , could be related to stabilization of the excited state. This behavior is mainly attributed to a strong ICT effect.^[22]

The Lippert–Mataga equation [Eq. (1)] is used to estimate the relationship between solvent polarity and the nature of the emission:

$$\Delta\nu = \nu_a - \nu_e = \frac{2\Delta f}{hca^2} (\mu_E - \mu_G)^2 + \text{const} \quad (1)$$

in which $\Delta\nu$ is the Stokes shift; ν_a is the maximum absorbance wavenumber; ν_e is the emission wavenumber; μ_G and μ_E are the dipole moments in the ground and excited states, respectively; and h , c , and a are the Planck constant, the speed of light, and the Onsager solvent cavity radius, respectively. The solvent polarity, Δf , is calculated by using Equation (2):

$$\Delta f = \frac{\varepsilon - 1}{2\varepsilon + 1} - \frac{n^2 - 1}{2n^2 + 1} \quad (2)$$

in which ε and n are the static dielectric constant and the refractive index of the solvent, respectively.

The relationship between $\Delta\nu$ with Δf is given in Figure 1 c and Figure S1 c in the Supporting Information. Both figures show that, with increasing solvent polarity (Δf), the Stokes shift ($\Delta\nu$) increases linearly. The results prove that IND-TPAT and IND-TPA exhibit solvatochromism effects. The steeper slope of IND-TPAT (5183.9 cm^{-1}) compared with that of IND-TPA (1263.7 cm^{-1}) indicates that the thiophene group of IND-

TPAT exhibits more remarkable solvatochromic effects than that of IND-TPA.

AIE properties

TPA is a typical ACQ core.^[10] Decorating TPA can probably change its emission behavior from ACQ to AIE,^[11] so it is necessary to investigate the AIE properties of IND-TPA and IND-TPAT. Thus, the fluorescent behavior of IND-TPA and IND-TPAT is recorded in a mixture of MeOH and water, both of which act as good and poor solvents for IND-TPA and IND-TPAT, respectively. As displayed in Figure 2a and c, in a dilute solution of MeOH (10 μM), IND-TPA and IND-TPAT show weak emissions and the PL spectroscopic lines are nearly parallel to the abscissa (Figure 2b and d). This could be ascribed to two reasons: hydrogen-bond formation with protic methanol,^[23] and the free rotation of carbon–nitrogen single bonds between the three phenyls and the nitrogen atom; these possibly eliminated the entire excited luminogens and eventually led to fluorescence quenching in dilute solutions in MeOH.^[24] If a large amount of water was added to the solution, the fluorescence was enhanced dramatically. When the water fraction (f_w) reached to 70 and 30%, respectively, the solutions of IND-TPA and IND-TPAT became more emissive. When the water fraction increased to 90%, the PL intensity was almost 200- and 14-fold stronger than that in pure MeOH. The strong fluorescence emission can be attributed to the aggregation of fluorogenic molecules: intramolecular rotations are restricted and hydrogen bonds are destroyed; this results in the AIE effect.^[5–7,25]

Theoretical calculations

To gain a deeper insight into the photophysical properties of IND-TPAT and IND-TPA, the electron-density distribution of the HOMO and LUMO of IND-TPAT and IND-TPA were calculated at the CAM-B3LYP/6-31G level (Gaussian 09). The simulation results of IND-TPAT and IND-TPA are shown in Figure 3. For both molecules, the HOMO electron clouds are mainly focused on the TPA core or 5-(4-diphenylaminophenyl)thiophene-2-carbal-

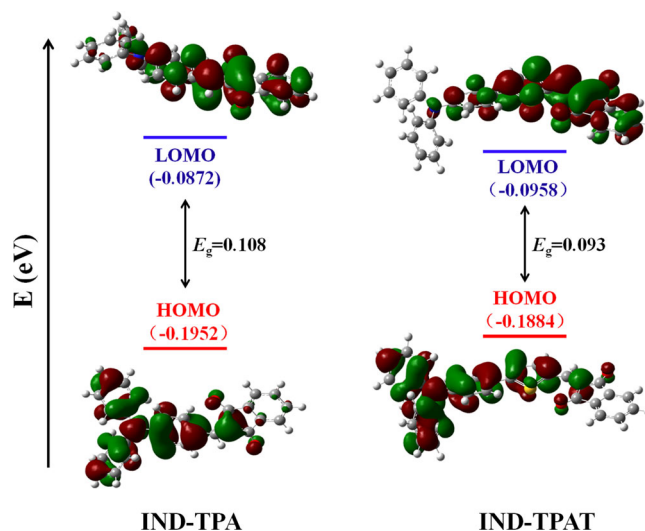


Figure 3. Calculated energy-level diagram of compounds IND-TPA and IND-TPAT.

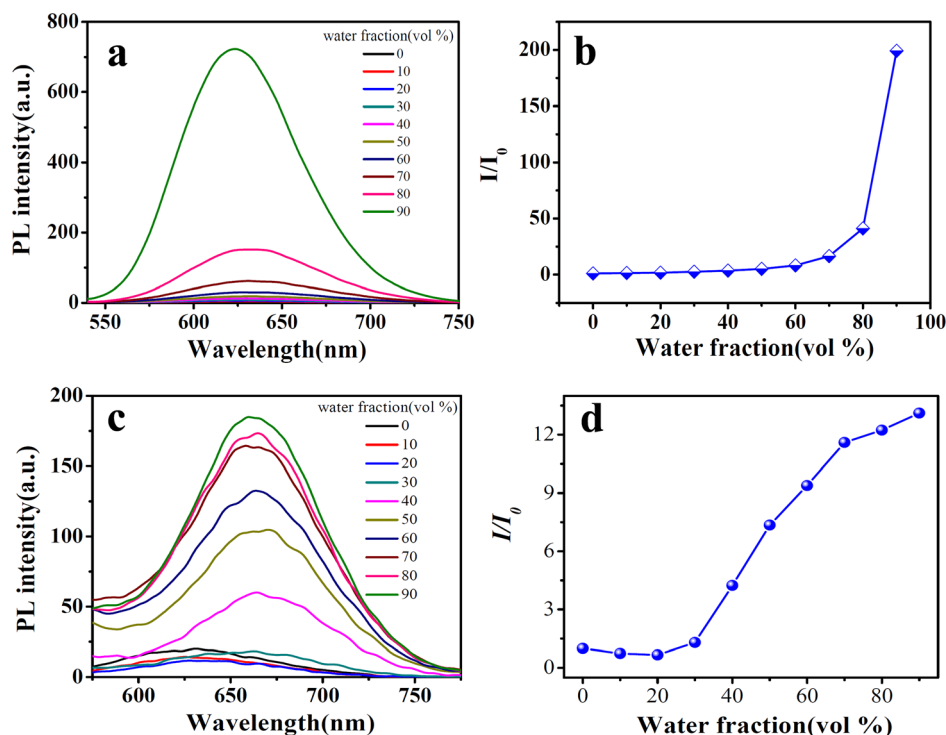


Figure 2. PL spectra of IND-TPA (a) and IND-TPAT (c) in mixtures of MeOH/water with different fractions of water (f_w); $c = 10 \mu\text{M}$, $\lambda_{\text{ex}} = 468 \text{ nm}$. Plot of the relative PL intensity (I/I_0) of IND-TPA (b) at $\lambda = 623 \text{ nm}$ and IND-TPAT (d) at $\lambda = 662 \text{ nm}$ versus the composition of the mixture of MeOH/water (f_w). I_0 = PL intensity of IND-TPA and IND-TPAT in MeOH, respectively.

dehyde (TPAT) segment, whereas the LUMO electron clouds are mainly concentrated on the electron-accepting IND section. Such electron distributions reveal the nature of the ICT phenomenon for IND-TPAT and IND-TPA. The energy gaps are calculated as $\Delta E_g = \text{HOMO} - \text{LUMO}$. The ΔE_g values of IND-TPAT and IND-TPA are 0.108 and 0.0958 eV, respectively. As exhibited in Figures S2 and S3 in the Supporting Information, there are planar configurations between the thienyl ring and IND (2 and 3 in Figure S2) of IND-TPAT and between the phenyl ring and IND (1 and 2 in Figure S3) of IND-TPA. Both dihedral angles are 0° , which is mainly due to the formation of an intramolecular hydrogen bond between the hydrogen atom of the phenyl ring and the carbonyl group of IND. In IND-TPAT, the phenyl and thienyl rings (1 and 2 in Figure S2 in the Supporting Information) have a less distorted configuration owing to steric repulsion between the hydrogen atom of the phenyl and thienyl rings, so the dihedral angle is 13° . Thus, relative to IND-TPA, IND-TPAT has greater conjugation and a smaller ΔE_g value. From the slope and Onsager cavity radius, dipole moment changes, between the ground and excited states of IND-TPA and IND-TPAT, are determined according to Equation (1) and the optimized structures in Figure 3. Assuming that the Onsager cavity radius, a , is given as $a = (3V_{\text{vdw}}/4\pi)^{1/3}$, in which V_{vdw} is the van der Waals volume of the solute,^[26] the cavity radius is determined to be 5.15 Å for IND-TPA and 5.38 Å for IND-TPAT. Thus, the dipole moment changes are calculated to be 4.05 D for IND-TPA and 8.75 D for IND-TPAT. The dipole moments of the excited state are 7.67 and 11.55 D, respectively. Such high

dipole moments for IND-TPA and IND-TPAT at the excited state must be important for solvatochromic fluorescence.

Piezochromic properties

We find that the emission colors of IND-TPAT and IND-TPA solids change when an external pressure exists. To evaluate the fluorescence emission performances of the powders before and after grinding, PL spectroscopy is applied (Figure 4). The emission wavelengths of powders as-prepared and after grinding are $\lambda = 629$ and 677 nm, respectively, for IND-TPAT (Figure 4a). This result demonstrates that IND-TPAT possesses a typical mechanochromism property. To further study the chromic effects of IND-TPAT, we determined the recyclability between two emission powders (Figure 4c and d). IND-TPAT and IND-TPA exhibit excellent recyclability after three grinding and heating cycles. In contrast to IND-TPAT, IND-TPA shows inconspicuous mechano- and thermochromatic properties. The as-prepared and ground powders are orange and light red under UV irradiation. The PL spectra (Figure 4b) show that after grinding the emission wavelength redshifts by only 21 nm (from $\lambda = 611$ to 632 nm). Although IND-TPA exhibits good repeatability between grinding and heating (Figure 4d), considering its inconspicuous colors, we conclude that the IND-TPA molecule is not a typical mechano- and thermochromism material. Meanwhile, the results prove that TPA, 4-formyltriphenylamine (TPAF), and TPAT have slight wavelength changes, only 3–4 nm redshifts occur after grinding (Figure S4 in the Sup-

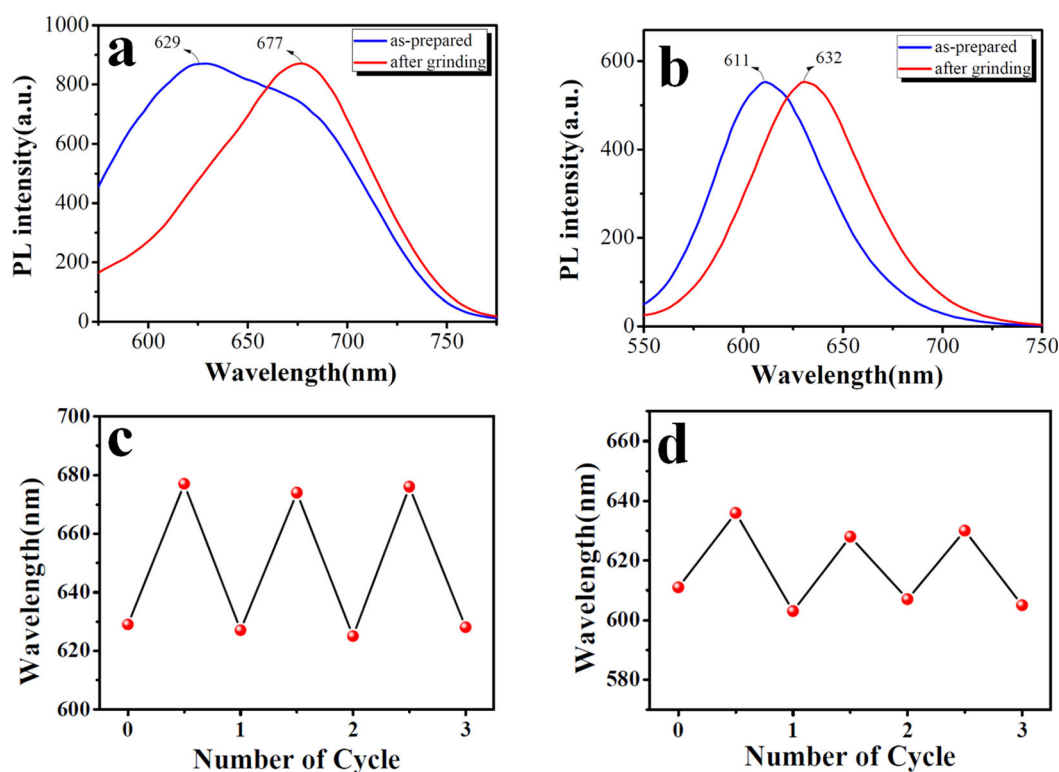


Figure 4. PL spectra of powders of IND-TPAT (a) and IND-TPA (b) as-prepared and after grinding, $\lambda_{\text{ex}} = 468$ nm. Reversible switching of the emission wavelengths of IND-TPAT (c) and IND-TPA (d) after repeated grinding and heating cycles. The heating temperature was 130°C .

porting Information). Thus, TPA, TPAF, and TPAT are not mechano- and thermochromism materials.

To further understand the piezochromic phenomenon, XRD analysis was performed on powders of IND-TPAT and IND-TPA. As shown in Figure 5, both solids display intensified and sharp diffraction peaks as-prepared, whereas after grinding most of the sharp peaks become weak, which reveals that the mechano-

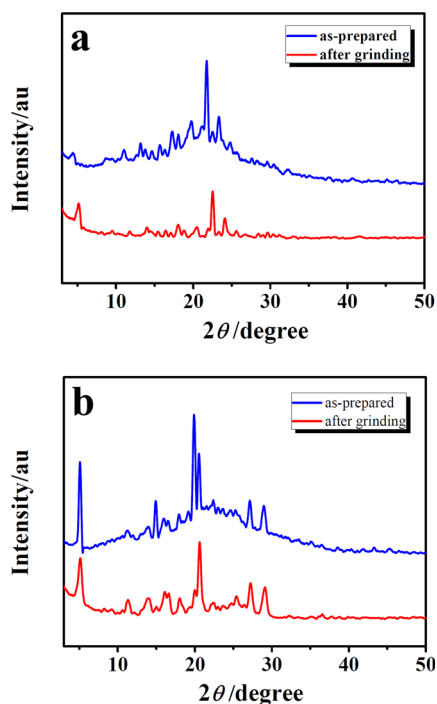


Figure 5. XRD patterns of IND-TPAT (a) and IND-TPA (b); blue lines indicate the as-prepared powders and the red lines indicate the ground samples.

chromism phenomenon results from the transformation between crystalline and amorphous states.^[4a] Thermal annealing is a helpful technique to reconstruct the crystalline structure. As shown in Figure 4c and d, both materials can be recycled many times. Thus, we infer that color changes under different conditions are induced by packing of the molecules. The pattern changes for IND-TPAT and IND-TPA were also studied by differential scanning calorimetry (DSC). The results in Figure S5 in the Supporting Information indicate that there are endothermic peaks at approximately 194 and 166 °C in the DSC curve of the initial powder. A new exothermic peak appears in the DSC curve of the ground powder. This new peak indicates the metastable amorphous state of the ground powder.

Responses to TBAF and TBAI

Highly selective detection of TBAF and tetrabutylammonium iodide (TBAI) over other potentially competing species is necessary. The selectivity of IND-TPAT and IND-TPA for different analytes was determined by fluorescence tests. Under the same conditions, we analyzed the fluorescence responses of IND-TPAT and IND-TPA towards analytes including adipic acid, ben-

zoic acid, trifluoroacetic acid (TFA), acetic acid, sodium ethoxide, sodium dodecyl benzene sulfonate (SDBS), potassium *tert*-butoxide (KTB), benzylamine, TBAF, tetrabutylammonium chloride, tetrabutylammonium bromide, and TBAI. Analytes are added to solutions of IND-TPAT and IND-TPA (2×10^{-5} M) in THF, and the emissions of IND-TPAT and IND-TPA are measured 1 h after the addition of analytes. As shown in Figure 6 and Fig-

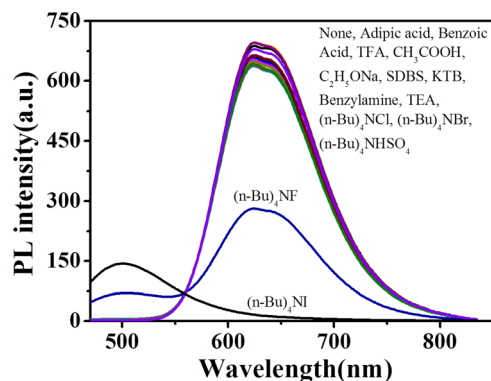


Figure 6. Fluorescence spectra of IND-TPAT (2×10^{-5} M, in THF) upon the addition of different analytes.

ure S6 in the Supporting Information, among the analytes studied, clear fluorescence quenching is observed upon the addition of five equivalents of TBAF and TBAI to IND-TPAT and IND-TPA at $\lambda_{\text{max}} = 625$ and 589 nm, respectively. Thus, the sensing behavior of IND-TPAT and IND-TPA to two kinds of tetrabutylammonium salts in THF were further investigated.

The fluorescence spectroscopy titrations were performed in THF at room temperature. As depicted in Figure 7 and Figure S7 in the Supporting Information, the fluorescence of IND-TPAT and IND-TPA changed in the presence of TBAF (a and b) and TBAI (c and d). The emission bands of IND-TPAT and IND-TPA at $\lambda_{\text{max}} = 625$ and 589 nm decrease gradually, whereas new emission bands at $\lambda_{\text{max}} = 500$ and 450 nm emerge and are enhanced gradually at the same time (Figure 7a,c and Figure S7a,c in the Supporting Information). From the results in Figure 7b,d and Figure S7b,d in the Supporting Information, the detection limits are calculated by the concentration of the sharp change in fluorescence intensity multiplied by the concentrations of IND-TPAT and IND-TPA.^[27] The following equation was used for to calculate the detection limit: $D_L = C_L C_T$ (C_L : concentrations of IND-TPAT and IND-TPA; C_T : concentrations of titrant at which the change is observed). Thus, IND-TPAT and IND-TPA possess the same detection limits of 2 and 1.2 ppb for F^- and I^- , respectively.

In addition, the colors of IND-TPAT and IND-TPA (in THF) changed from red to green and yellow to blue (Figures S8 and S9 in the Supporting Information), and could be detected by the naked eye. Take the detection of TBAF as an example, a clear relationship between PL intensity and time is recorded in Figure 8 and Figure S10 in the Supporting Information. As shown in Figure 8 and Figure S10 in the Supporting Information, solutions of IND-TPAT and IND-TPA emitted at $\lambda = 625$ and

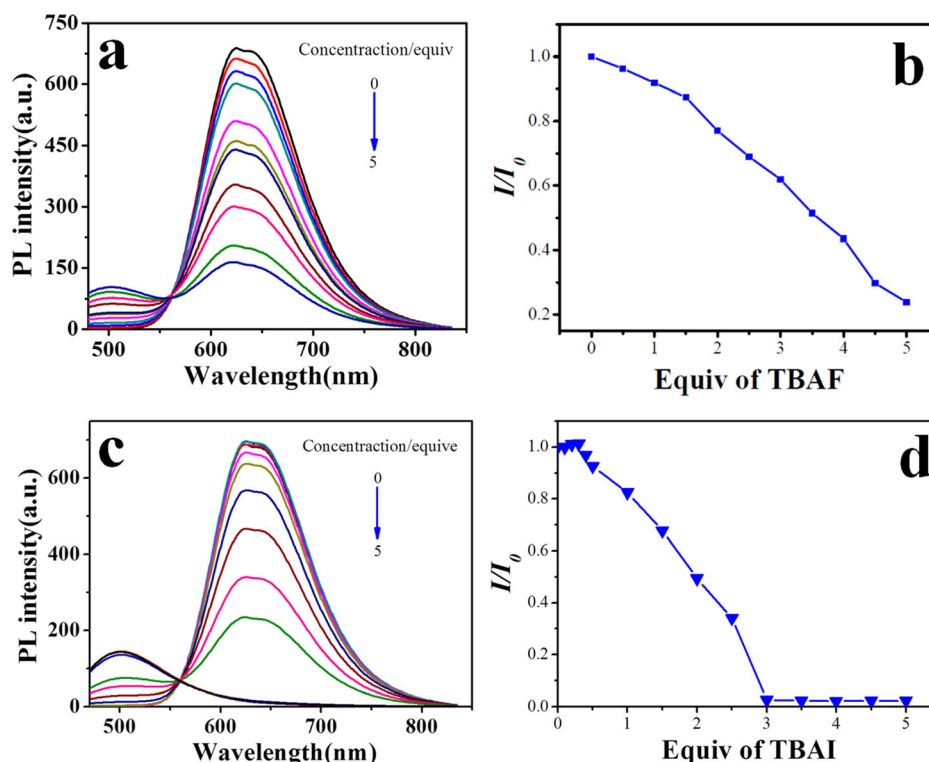


Figure 7. Fluorescence spectra of IND-TPAT upon titration with solutions of TBAF (a) and TBAI (c) in THF. A plot of changes of fluorescence intensity upon the addition of TBAF (b) and TBAI (d) at $\lambda = 625$ nm.

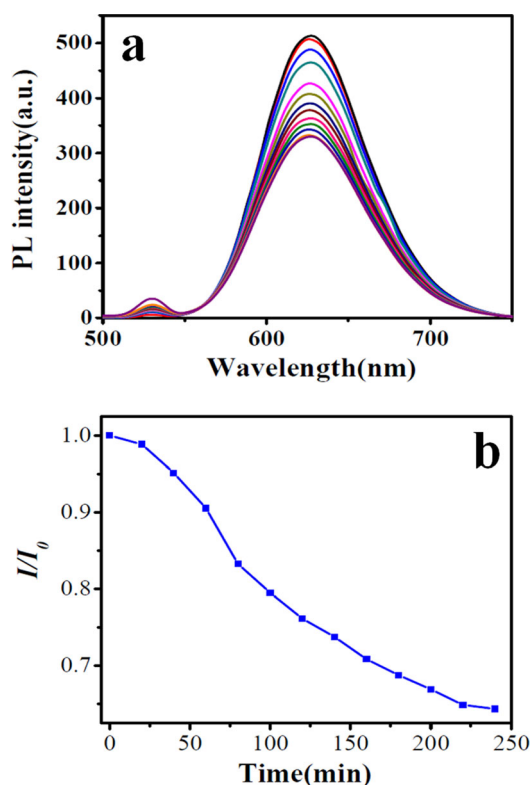


Figure 8. a) Time-dependent PL intensity changes to IND-TPAT in THF. b) Variation of the band intensity of the emission of IND-TPAT versus reaction time. The data are extracted from a). I_0 : the initial intensity of IND-TPAT in THF; I : the PL intensity of the addition of TBAF (5 equiv) in solution at different reaction times. Concentration of IND-TPAT: $20 \mu\text{M}$; $\lambda_{\text{ex}} = 468$ nm. The solution was recorded every 20 min.

589 nm in the first stage, and as the reaction time increased, the fluorescence was clearly quenched. The relative fluorescence quantum yields of IND-TPAT and IND-TPA are 1.4 and 0.8%, respectively. After the addition of TBAF (5 equiv), the relative fluorescence quantum yields of IND-TPAT and IND-TPA are enhanced to 72 and 14%, respectively.

To further understand the practical applicability of IND-TPAT and IND-TPA as TBAF and TBAI probes, interference experiments were performed by fluorescence spectroscopy. The emission intensities of IND-TPAT and IND-TPA in the presence of five equivalents of F^- and I^- remained unaffected upon the addition of five equivalents of competing molecules. (Figures 9 and 10 and Figures S11 and S12 in the Supporting Information).

To further verify the reaction mechanism, ^1H NMR titration analysis of IND-TPAT and IND-TPA was performed in CDCl_3 with varying equivalents of TBAF (Figure 11 and Figure S13 in the Supporting Information) and TBAI (Figures S14 and S15 in the Supporting Information). Notably, with the addition of TBAF (0–4 equiv) to solutions of IND-TPAT and IND-TPA, the resonance corresponding to the aldehyde hydrogen emerged; this was probably produced in the hydrolysis of IND-TPAT and IND-TPA by TBAF^[4a] (Scheme 2 and Scheme S2 in the Supporting Information). Meanwhile, the resonances of aromatic protons continually shift upfield with the addition of fluoride ions. Consequently, the results of the ^1H NMR titration provide strong evidence for the proposed mechanism depicted in Scheme 2. For TBAI, the resonance protons continually shift upfield with the addition of iodide ions. As previously reported,^[29] the

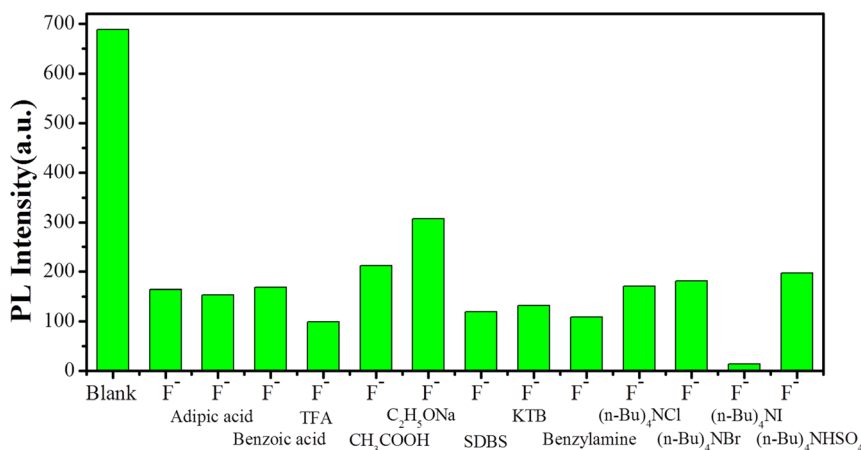


Figure 9. Competitive selectivity of IND-TPAT towards TBAF in the presence of other analytes (5 equiv) at $\lambda = 625$ nm.

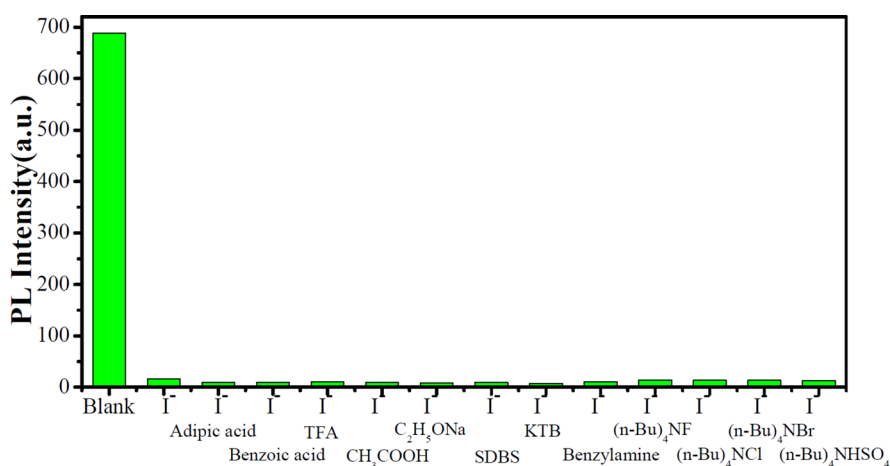


Figure 10. Competitive selectivity of IND-TPAT towards TBAI in the presence of other analytes (5 equiv) at $\lambda = 625$ nm.

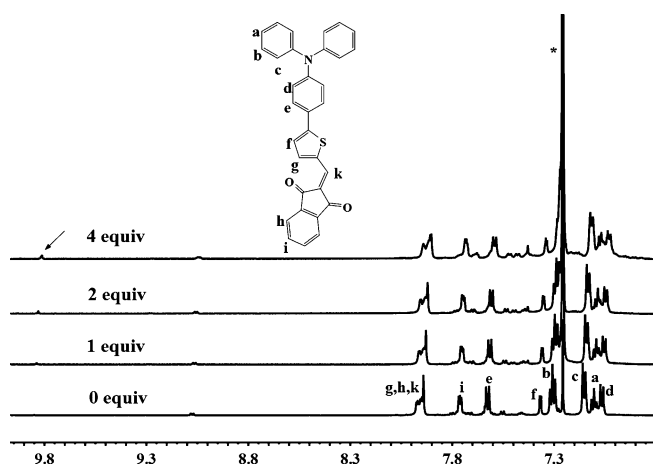
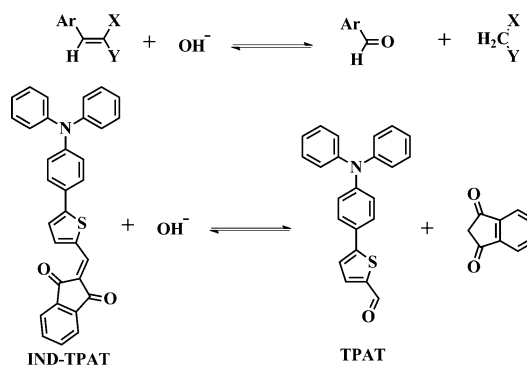


Figure 11. ^1H NMR spectroscopic changes of IND-TPAT in CDCl_3 in the presence of TBAF (0–4 equiv; δ/ppm).



Scheme 2. The hydroxyl mechanism of IND-TPAT in THF in the presence of TBAF.

charge-transfer complex may be responsible for this phenomenon. The heavy-atom interaction between the excited state of IND-TPAT (or IND-TPA) and iodides leads to an enhancement of

the spin-orbit coupling. Here, the heavy-atom effect is caused by the formation of a weak, transient, probably charge-transfer complex between the TPA moieties in IND-TPAT (or IND-TPA) and the iodide ions.

Conclusion

It was demonstrated that two representative red-emitting TPA-based derivatives, IND-TPAT and IND-TPA, were synthesized. Both derivatives demonstrated evident AIE properties, solvatochromism effects, and piezochromic behavior. The XRD and cycle measurements reveal that the piezochromic property is mainly caused by a transition from crystalline to an amorphous phase. In addition, IND-TPAT and IND-TPA could be used as fluorescence probes to detect F^- and I^- sensitively; detection could even be performed by the naked eye. Furthermore, our work explored a new strategy to synthesize red and near-infrared materials with piezochromic performances. Further research into synthetic protocols and applications is underway.

Experimental Section

Synthesis and characterization of IND-TPAT and IND-TPA

5-(4-Diphenylaminophenyl)thiophene-2-carbaldehyde (TPAT) was synthesized by 4-bromophenyl)diphenylamine Suzuki coupling with 5-formylthiophene-2-boronic acid. TPAF was prepared according to the Vilsmeier–Haack reaction. IND-TPAT and IND-TPA were synthesized from the precursor TPAT and TPAF through Knoevenagel condensation with IND (Scheme 1).^[28] The obtained compounds were characterized by 1H NMR, ^{13}C NMR, and FTIR spectroscopy (see the Supporting Information).

Instrumentation

1H (600 MHz) and ^{13}C NMR (100 MHz) spectra were recorded on a Mercury spectrometer at 25 °C. UV/Vis absorption spectra were recorded on a TU-1901 spectrometer from $\lambda = 190$ to 1100 nm. Fluorescence spectra were measured by using a PE LS-55 luminescence/fluorescence spectrophotometer. FTIR spectra were recorded on a DIGIL FTS3000 spectrophotometer as KBr pellets. XRD patterns of IND-TPAT and IND-TPA were examined on a Phillips diffractometer by using Ni-filtered $Cu_{K\alpha}$ radiation.

Acknowledgements

This study was supported by the National Natural Science Foundation of China (nos. 21202133 and 21361023). We thank the Key Laboratory of Eco-Environment-Related Polymer Materials (Northwest Normal University) and The Ministry of Education Scholars Innovation Team (IRT 1177) for financial support. We also thank the Analytical and Testing Centre of Northwest Normal University for related analysis.

Keywords: aggregation · conjugation · luminescence · piezochromism · sensors

- [1] a) Z. Wang, T. Y. Yong, J. Wan, Z. H. Li, H. Zhao, Y. Zhao, L. Gan, X. L. Yang, H. B. Xu, C. Zhang, *ACS Appl. Mater. Interfaces* **2015**, *7*, 3420–3425; b) Z. Li, C. S. Theile, G. Y. Chen, A. M. Bilate, J. N. Duarte, A. M. Avalos, T. Fang, R. Barberena, S. Sato, H. L. Ploegh, *Angew. Chem. Int. Ed.* **2015**, *54*, 11706–11710; *Angew. Chem.* **2015**, *127*, 11872–11876; c) Z. Wang, S. Chen, J. W. Lam, W. Qin, R. T. Kwok, N. Xie, Q. Hu, B. Z. Tang, *J. Am. Chem. Soc.* **2013**, *135*, 8238–8245; d) H. C. Ma, C. X. Qi, C. Cheng,

- Z. M. Yang, H. Y. Cao, Z. W. Yang, J. H. Tong, X. Q. Yao, Z. Q. Lei, *ACS Appl. Mater. Interfaces* **2016**, *8*, 8341–8348.
- [2] a) R. Zhang, Y. Yuan, J. Liang, R. T. Kwok, Q. Zhu, G. Feng, J. Geng, B. Z. Tang, B. Liu, *ACS Appl. Mater. Interfaces* **2014**, *6*, 14302–14310; b) X. Lu, W. Wang, Q. Dong, X. Bao, X.; Lin, W. Zhang, X. Dong, W. Zhao, *Chem. Commun.* **2015**, *51*, 1498–1501; c) Y. Zhang, X. Shao, Y. Wang, F. Pan, R. Kang, F. Peng, Z. Huang, W. Zhang, W. Zhao, *Chem. Commun.* **2015**, *51*, 4245–4248; d) N. Zhao, J. W. Lam, H. H. Sung, H. M. Su, I. D. Williams, K. S. Wong, B. Z. Tang, *Chem. Eur. J.* **2014**, *20*, 133–138; e) A. Fermi, G. Bergamini, M. Roy, M. Gingras, P. Ceroni, *J. Am. Chem. Soc.* **2014**, *136*, 6395–6400; f) Q. K. Qi, J. Y. Qian, S. Q. Ma, B. Xu, S. X. A. Zhang, W. J. Tian, *Chem. Eur. J.* **2015**, *21*, 1149–1155.
- [3] a) L. Yao, S. Zhang, R. Wang, W. Li, F. Shen, B. Yang, Y. Ma, *Angew. Chem. Int. Ed.* **2014**, *53*, 2119–2123; *Angew. Chem.* **2014**, *126*, 2151–2155; b) W. Qin, J. W. Lam, Z. Yang, S. Chen, G. Liang, W. Zhao, H. S. Kwok, B. Z. Tang, *Chem. Commun.* **2015**, *51*, 7321–7324; c) J. Huang, R. Tang, T. Zhang, Q. Li, G. Yu, S. Xie, Y. Liu, S. Ye, J. Qin, Z. Li, *Chem. Eur. J.* **2014**, *20*, 5317–5326; d) J. J. McDowell, D. Gao, D. S. Seferos, G. Ozin, *Polym. Chem.* **2015**, *6*, 3781–3789.
- [4] a) J. Tong, Y. Wang, J. Mei, J. Wang, A. Qin, J. Z. Sun, B. Z. Tang, *Chem. Eur. J.* **2014**, *20*, 4661–4670; b) S. Kohmoto, T. Chuko, S. Hisamatsu, Y. Okuda, H. Masu, M. Takahashi, K. Kishikawa, *Cryst. Growth Des.* **2015**, *15*, 2723–2731; c) T. T. Tasso, T. Furuyama, N. Kobayashi, *Chem. Eur. J.* **2015**, *21*, 4817–4824; d) G. R. Krishna, M. S. R. N. Kiran, C. L. Fraser, U. Ramamurthy, C. M. Reddy, *Adv. Funct. Mater.* **2013**, *23*, 1422–1430; e) X. Luo, J. Li, C. Li, L. Heng, Y. Q. Dong, Z. Liu, Z. Bo, B. Z. Tang, *Adv. Mater.* **2011**, *23*, 3261–3265; f) C. Niu, Y. You, L. Zhao, D. He, N. Na, J. Ouyang, *Chem. Eur. J.* **2015**, *21*, 13983–13990; g) Q. K. Qi, J. Y. Qian, X. Tan, J. B. Zhang, L. J. Wang, B. Xu, B. Zou, W. J. Tian, *Adv. Funct. Mater.* **2015**, *25*, 4005–4010; h) Q. K. Qi, J. B. Zhang, B. Xu, B. Li, S. X. A. Zhang, W. J. Tian, *J. Phys. Chem. C* **2013**, *117*, 24997–25003.
- [5] Y. Hong, J. W. Y. Lam, B. Z. Tang, *Chem. Soc. Rev.* **2011**, *40*, 5361–5388.
- [6] J. Luo, Z. Xie, J. W. Y. Lam, L. Cheng, B. Z. Tang, H. Chen, C. Qiu, H. S. Kwok, X. Zhan, Y. Liu, D. Zhu, *Chem. Commun.* **2001**, 1740–1741.
- [7] a) Y. Hong, J. W. Lam, B. Z. Tang, *Chem. Commun.* **2009**, 4332–4353; b) J. Chen, C. C. W. Law, J. W. Y. Lam, Y. Dong, S. M. F. Lo, I. D. Williams, D. Zhu, B. Z. Tang, *Chem. Mater.* **2003**, *15*, 1535–1546.
- [8] a) Z. Chi, X. Zhang, B. Xu, X. Zhou, C. Ma, Y. Zhang, S. Liu, J. Xu, *Chem. Soc. Rev.* **2012**, *41*, 3878–3896; b) S. Varughese, *J. Mater. Chem. C* **2014**, *2*, 3499–3516; c) X. Zhang, Z. Chi, Y. Zhang, S. Liu, J. Xu, *J. Mater. Chem. C* **2013**, *1*, 3376–3390.
- [9] a) S. J. Lim, B. K. An, S. D. Jung, M. A. Chung, S. Y. Park, *Angew. Chem. Int. Ed.* **2004**, *43*, 6346–6350; *Angew. Chem.* **2004**, *116*, 6506–6510; b) C. Dou, D. Chen, J. Iqbal, Y. Yuan, H. Zhang, Y. Wang, *Langmuir* **2011**, *27*, 6323–6329.
- [10] W. Z. Yuan, P. Lu, S. Chen, J. W. Lam, Z. Wang, Y. Liu, H. S. Kwok, Y. Ma, B. Z. Tang, *Adv. Mater.* **2010**, *22*, 2159–2163.
- [11] a) H. Ma, C. Qi, H. Cao, Z. Zhang, Z. Yang, B. Zhang, C. Chen, Z. Q. Lei, *Chem. Asian J.* **2016**, *11*, 58–63; b) Y. Ma, H. Ma, Z. Yang, J. Ma, Y. Su, W. Li, Z. Lei, *Langmuir* **2015**, *31*, 4916–4923.
- [12] a) M. Kleerekoper, *Endocrinol. Metab. Clin. North Am.* **1998**, *27*, 441–452; b) X. Zheng, W. Zhu, D. Liu, H. Ai, Y. Huang, Z. Lu, *ACS Appl. Mater. Interfaces* **2014**, *6*, 7996–8000; c) S. Mohapatra, S. Sahu, S. Nayak, S. K. Ghosh, *Langmuir* **2015**, *31*, 8111–8120.
- [13] a) S. Ayoob, A. K. Gupta, *Crit. Rev. Environ. Sci. Technol.* **2006**, *36*, 433–487; b) P. Singh, M. Barjatiya, S. Dhing, R. Bhatnagar, S. Kothari, V. Dhar, *Urol. Res.* **2001**, *29*, 238–244.
- [14] a) F. Han, Y. Bao, Z. Yang, T. M. Fyles, J. Zhao, X. Peng, J. Fan, Y. Wu, S. Sun, *Chem. Eur. J.* **2007**, *13*, 2880–2892; b) R. Hu, J. Feng, D. Hu, S. Wang, S. Li, Y. Li, G. Yang, *Angew. Chem. Int. Ed.* **2010**, *49*, 4915–4918; *Angew. Chem.* **2010**, *122*, 5035–5038; c) J. A. Gu, V. Mani, S. T. Huang, *Analyst* **2015**, *140*, 346–352.
- [15] a) B. Ke, W. Chen, N. Ni, Y. Cheng, C. Dai, H. Dinh, B. Wang, *Chem. Commun.* **2013**, 49, 2494–2496; b) M. Cametti, K. Rissanen, *Chem. Commun.* **2009**, 2809–2829.
- [16] a) X. Cheng, S. Li, G. Xu, C. Li, J. Qin, Z. Li, *ChemPlusChem* **2012**, *77*, 908–913; b) A. Lafleur-Lambert, J. B. Giguère, J. F. Morin, *Macromolecules* **2015**, *48*, 8376–8381.
- [17] a) Q. Wang, Y. Xie, Y. Ding, X. Li, W. Zhu, *Chem. Commun.* **2010**, 46, 3669–3671; b) Y. Zhou, J. F. Zhang, J. Yoon, *Chem. Rev.* **2014**, *114*, 5511–5571.

- [18] a) Y. Bao, B. Liu, H. Wang, J. Tian, R. Bai, *Chem. Commun.* **2011**, 47, 3957–3959; b) L. Gai, H. Chen, B. Zou, H. Lu, G. Lai, Z. Li, Z. Shen, *Chem. Commun.* **2012**, 48, 10721–10723.
- [19] a) S. Y. Kim, J. I. Hong, *Org. Lett.* **2007**, 9, 3109–3112; b) T. Neumann, Y. Dienes, T. Baumgartner, *Org. Lett.* **2006**, 8, 495–497.
- [20] H. A. Ho, M. Leclerc, *J. Am. Chem. Soc.* **2003**, 125, 4412–4413.
- [21] a) C. Reichardt, *Chem. Rev.* **1994**, 94, 2319–2358; b) J. Mei, J. Wang, J. Z. Sun, H. Zhao, W. Yuan, C. Deng, S. Chen, H. H. Y. Sung, P. Lu, A. Qin, H. S. Kwok, Y. Ma, I. D. Williams, B. Z. Tang, *Chem. Sci.* **2012**, 3, 549–558; c) J. Lee, H. T. Chang, H. An, S. Ahn, J. Shim, J.-M. Kim, *Nat. Commun.* **2013**, 4, 2461.
- [22] a) W. Rettig, *Angew. Chem. Int. Ed. Engl.* **1986**, 25, 971–988; *Angew. Chem.* **1986**, 98, 969–986; b) G. Qian, B. Dai, M. Luo, D. B. Yu, J. Zhan, Z. Q. Zhang, D. G. Ma, Z. Y. Wang, *Chem. Mater.* **2008**, 20, 6208–6216.
- [23] K. Mizuguchi, H. Kageyama, H. Nakano, *Mater. Lett.* **2011**, 65, 2658–2661.
- [24] a) C. Coluccini, A. K. Sharma, D. Merli, D. V. Griend, B. Mannucci, D. Pasini, *Dalton Trans.* **2011**, 40, 11719–11725; b) C. Coluccini, A. K. Sharma, M. Caricato, A. Sironi, E. Cariati, S. Righetto, E. Tordin, C. Botta, A. Forni, D. Pasini, *Phys. Chem. Chem. Phys.* **2013**, 15, 1666–1674.
- [25] a) J. W. Chen, B. Xu, X. Y. Ouyang, B. Z. Tang, Y. Cao, *J. Phys. Chem. A* **2004**, 108, 7522–7526; b) Y. Ren, J. W. Y. Lam, Y. Q. Dong, B. Z. Tang, K. S. Wong, *J. Phys. Chem. B* **2005**, 109, 1135–1140.
- [26] F. H. A. Rummens, *Can. J. Chem.* **1976**, 54, 254–269.
- [27] V. Bhalla, A. Gupta, M. Kumar, *Org. Lett.* **2012**, 14, 3112–3115.
- [28] C. H. Yang, W. C. Lin, T. L. Wang, Y. T. Shieh, W. J. Chen, S. H. Liao, Y. K. Sun, *Mater. Chem. Phys.* **2011**, 130, 635–643.
- [29] M. Vetrichelvan, R. Nagarajan, S. Valiyaveetil, *Macromolecules* **2006**, 39, 8303–8310.

Manuscript received: April 25, 2016

Accepted Article published: May 25, 2016

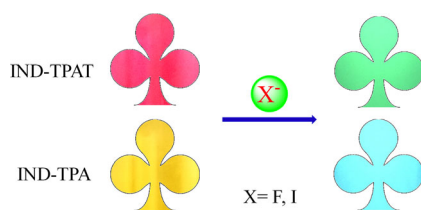
Final Article published: ■ ■ ■, 0000

FULL PAPERS

C. Qi, H. Ma,* H. Fan, Z. Yang, H. Cao,
Q. Wei, Z. Lei*



**Study of Red-Emission Piezochromic
Materials Based on Triphenylamine**



Seeing red: Two conjugated molecules based on triphenylamine (TPA) and 1,3-indandione (IND) are prepared by employing Suzuki cross-coupling reaction and Knoevenagel condensation. Both materials demonstrate red emission, aggregation-induced emission behavior, and solvatochromic and piezochromic properties. These red luminescence materials are able to respond to fluoride and iodide in THF sensitively (see figure; TPAT = 5-(4-diphenylaminophenyl)thiophene-2-carbaldehyde).